

Selecting Materials for Radiation Balanced Lasers

Steven R. Bowman

*Photonics Technology Branch, Naval Research Laboratory
Washington, D.C. 20375-5320
bowman@ccf.nrl.navy.mil*

Carl E. Mungan

*Department of Physics, The University of West Florida
Pensacola, FL 32514-5751
cmungan@uwf.edu*

Abstract: Well-characterized solid-state laser materials are evaluated for performance in radiation balanced laser systems. New figures-of-merit are developed and applied to ytterbium doped materials. Superior performance is predicted for high cross section tungstate materials. Photothermal deflection experiments on samples of Yb³⁺ doped KGd(WO₄)₂ confirm anti-Stokes fluorescence cooling. Observations of optical cooling in this high figure-of-merit material confirm the potential of this approach for laser power scaling.

OCIS Codes: (140.3580) Lasers, solid-state, (140.3380) Laser materials, (140.3320) Laser cooling

Introduction

The physical mechanism of radiation cooling by anti-Stokes fluorescence was originally proposed in 1929 [1]. It can be easily understood. Absorption of a photon can temporarily push an atom away from thermal equilibrium with its surroundings. If the atom then spontaneously emits after thermal equilibrium has been re-established, any frequency shift in the fluorescence compared to the absorbed radiation results in a net heating or cooling of the material. While simple in concept, to obtain radiative cooling in practice requires materials with near unity fluorescence efficiency. Anti-Stokes cooling was first reported in 1981 for CO₂ gas [2], in 1995 and 1996 for organic dye solutions [3,4], and in 1995 for ytterbium doped ZBLANP glass [5,6].

It has been proposed that solid-state lasers could be constructed in which the cooling of anti-Stokes fluorescence would offset heat generated by stimulated emission [7]. This mode of laser operation is referred to as radiation balanced (RB) lasing. Unlike conventional exothermic laser systems, RB lasers would exhibit little or no internal heat generation. In principle, this technique would allow RB lasers to be scaled up to much higher average powers than conventional solid-state laser systems. In this paper, we evaluate a range of well-characterized ytterbium doped laser materials for operation as RB lasers. Crystalline hosts are emphasized instead of glasses because of their generally higher cross sections and well-defined micro-environments. Optical cooling experiments on a few materials confirm the potential of this approach.

Steady State Radiation Balanced Lasing

For ytterbium doped materials, the process of RB lasing begins with absorption at the pump wavelength, λ_p , near 1.0 μm . This excites trivalent ytterbium ions from the $^2F_{7/2}$ ground state to the $^2F_{5/2}$ excited state. Both of these states are Stark split into several closely spaced energy levels. The picosecond timescale for phonon coupling of these levels to the lattice combined with the millisecond spontaneous lifetime ensure Boltzmann distributions for both of the $(2J+1)/2$ multiplets. At any particular temperature, this equilibrium distribution can be conveniently expressed in terms of the effective cross sections for absorption, $\sigma_A(\lambda)$, and emission $\sigma_E(\lambda)$ by the relation

$$\beta(\lambda) \equiv \frac{\sigma_A(\lambda)}{\sigma_A(\lambda) + \sigma_E(\lambda)}. \quad (1)$$

Spontaneous emission of the $^2F_{5/2}$ excited state occurs in a time τ and yields a broadband fluorescence spectra $I_F(\lambda)$ with a mean wavelength of

$$\lambda_F = \frac{\int I_F(\lambda) \lambda d\lambda}{\int I_F(\lambda) d\lambda}. \quad (2)$$

In the absence of radiative trapping or quenching, a red shift of the pump from the mean wavelength will result in a net cooling of the material. Under appropriate conditions, laser emission can occur at λ_L , usually near 1.03 μm . If the pump wavelength satisfies the condition

$$\lambda_F \leq \lambda_p \leq \lambda_L, \quad (3)$$

then radiation balance can occur. Radiation balance describes the condition when the absorbed power density matches the radiated power density at each point within the mode volume. This balance can be established and maintained through control of the pump intensity, I_p , and laser intensity, I_L [7]. For materials with near unity fluorescence yield, steady state RB will occur when these intensities satisfy

$$\frac{I_L}{I_{L_{\text{sat}}}} = \left[1 - \frac{\beta(\lambda_L)}{\beta(\lambda_p)} \left(1 + \frac{I_{p_{\text{sat}}}}{I_p} \right) \right]^{-1} \quad (4)$$

where the RB saturation intensities $I_{L_{\text{sat}}}$ and $I_{p_{\text{sat}}}$ are defined as

$$I_{p_{\text{sat}}} = \frac{hc}{\lambda_F \tau \sigma_A(\lambda_p)} \frac{\lambda_L - \lambda_F}{\lambda_L - \lambda_p} \beta(\lambda_p) \quad \text{and} \quad I_{L_{\text{sat}}} = \frac{hc}{\lambda_F \tau \sigma_A(\lambda_L)} \frac{\lambda_p - \lambda_F}{\lambda_L - \lambda_p} \beta(\lambda_L). \quad (5)$$

As the intensities get large, Eq. 4 leads to minimum values for the pump and laser intensities that satisfy the RB condition:

$$I_{p_{\text{min}}} = \frac{\beta(\lambda_L)}{\beta(\lambda_p) - \beta(\lambda_L)} I_{p_{\text{sat}}} \quad \text{and} \quad I_{L_{\text{min}}} = \frac{\beta(\lambda_p)}{\beta(\lambda_p) - \beta(\lambda_L)} I_{L_{\text{sat}}}. \quad (6)$$

With the above relations, it is easy to show that the internal optical efficiency, η_o , for a cw RB laser must be simply

$$\eta_o = \frac{\lambda_p - \lambda_f}{\lambda_L - \lambda_f}. \quad (7)$$

Including the effects of pump saturation in a system with an active ion density of N_T , a simple expression can also be derived for the optical coupling efficiency per unit length, η_L , in cw RB lasers

$$\eta_L(\lambda_p, \lambda_L, I_p) \equiv \frac{1}{I_p} \frac{\partial I_L}{\partial z} = \sigma_A(\lambda_p) N_T \eta_o \frac{\beta(\lambda_p) - \beta(\lambda_L)}{\beta(\lambda_p)}. \quad (8)$$

Finally, like any other quasi-two level laser, the maximum small-signal gain coefficient, g_{\max} , which occurs for very high pump intensities can be written as

$$g_{\max} = \sigma_A(\lambda_L) N_T \frac{\beta(\lambda_p) - \beta(\lambda_L)}{\beta(\lambda_L)}. \quad (9)$$

Using the above steady state analysis, we can predict and compare RB laser performance for different materials. The first step is to identify the correct operating wavelengths for each material. In order to optimize both gain and efficiency for each material, we select the laser wavelength, λ_{OL} , and pump wavelength, λ_{OP} , that maximize the product of g_{\max} and η_L . This procedure gives unambiguous optimal values for both wavelengths. Once these optimum wavelengths are found, different materials can be compared using the following figures-of-merit:

$$F_{\text{eff}} \equiv \sigma_A(\lambda_{OP}) \frac{\beta(\lambda_{OP}) - \beta(\lambda_{OL})}{\beta(\lambda_{OP})} \frac{\lambda_{OP} - \lambda_f}{\lambda_{OL} - \lambda_f} \quad (10)$$

and

$$F_{\text{gain}} \equiv \sigma_A(\lambda_{OL}) \frac{\beta(\lambda_{OP}) - \beta(\lambda_{OL})}{\beta(\lambda_{OL})}. \quad (11)$$

Materials with high values of F_{eff} and F_{gain} should exhibit superior performance as radiation balanced lasers.

The optimization scheme described above is convenient and robust for a broad range of materials. It gives a good compromise between best efficiency and best gain. In practice however, a laser designer may elect to minimize the required pump intensity in order to facilitate construction of the pump source. Alternatively, one may choose to increase the separation between pump and laser wavelengths to facilitate optical coatings or optimize the laser for best gain. The impact of shifting the operating wavelengths varies substantially from one laser material to another. In the next section, we will use Eqs. 10 and 11 to compare some well-known ytterbium doped materials.

Ytterbium Doped RB Laser Materials

The figures-of-merit developed in the previous section can be immediately computed for any material and temperature from precise absorption and emission cross section spectra. However, since these figures-of-merit are quite sensitive to weak absorption in the long wavelength wings, it is often preferable to use the reciprocity principle for the calculations. If the energy levels of the upper and lower manifolds are known, then the red wing of the absorption cross section can usually be more accurately calculated from the emission data. Also the $\beta(\lambda)$ functions can be computed directly using

$$\beta(\lambda) = \left[1 + \frac{Z_1}{Z_2} \exp\left(\frac{\epsilon_2}{kT} - \frac{hc}{\lambda kT}\right) \right]^{-1}. \quad (12)$$

Here Z_2 and Z_1 are the thermal partition functions of the upper and lower states, and ϵ_2 is the energy difference between the lowest levels in these two states.

Host	λ_F	λ_{OP}	λ_{OL}	η_o	τ	I_{Pmin}	I_{Lmin}	Z_1/Z_2	F_{eff}	F_{gain}	Ref.
	nm (polarization)			%	ms	kW/cm ²		at 295 K	10 ⁻²² cm ²		
KY(WO ₄) ₂	992	002(a)	041(b)	20	0.60	1.6	5.5	1.23	41	36	8-10
KGd(WO ₄) ₂	993	001(a)	042(b)	17	0.60	1.3	4.3	1.23	36	37	8-10
Lu ₃ Al ₅ O ₁₂	1002	033	048	67	0.92	26	303	0.89	5.1	0.83	11
Sr ₅ (VO ₄) ₃ F	1041	047(π)	117(π)	8	0.59	0.14	1.6	1	5.8	9.2	12-13
Ca ₅ (PO ₄) ₃ F	1033	046(π)	123(π)	14	1.10	0.14	2.9	1	3.8	4.6	14
Y ₃ Al ₅ O ₁₂	1007	031	049	56	0.95	15	133	0.88	4.3	1.1	15
BaCaBO ₃ F	1020	035(π)	084(σ)	22	1.17	1.7	20	1	2.1	1.9	16
Y ₂ SiO ₅	1001	007(x)	036(y)	18	1.04	11	18	1	2.8	5.5	17
BaY ₂ F ₈	995	015(y)	030(y)	58	2.04	51	97	1	2.3	1.8	17
Sc ₂ O ₃	1022	042	095	27	0.80	2.3	34	1	1.25	1.0	18
KY ₃ F ₁₀	992	003	014	49	1.87	63	64	1	2.0	3.0	17
YAl ₃ (BO ₃) ₄	999	008(σ)	037(σ)	22	0.68	21	13	1.19	2.1	12	18
LiYF ₄	996	004(π)	017(π)	41	2.21	34	19	0.90	2.0	6.0	17
Ca ₂ Al ₂ SiO ₇	1012	028(σ)	081(σ)	22	0.82	4.7	16	1.17	1.02	3.0	20
ZBLANP	995	005	024	36	1.70	38	46	1.07	1.32	2.4	6
Ca ₄ GdO(BO ₃) ₃	1011	032(z)	083(x)	30	2.50	2.5	35	1.18	0.84	0.54	21
Rb ₂ NaYF ₆	996	011	068	20	10.8	1.8	17	1	0.25	0.34	17
YCa ₄ O(BO ₃) ₃	1035	047(z)	084(x)	25	2.28	8.9	15	0.96	0.21	0.63	22

Table 1. Parameters characterizing optimal RB lasing of 18 different Yb³⁺ doped materials.

Table 1 details the eighteen different ytterbium doped laser materials included in this study. Emission and absorption spectral data for each material were digitized from previous reports in the literature [6,8-22]. Reported values of the energy levels within the ²F_{7/2} ground state and the ²F_{5/2} excited state were used to compute the partition and $\beta(\lambda)$ functions. When necessary, emission spectra were scaled to effective cross sections through comparison with the reciprocity calculated wing emission. The scale of each emission spectrum was checked with the reported fluorescence lifetime via the Füchtbauer-Ladenburg equation. Where possible, carefully measured laser absorption coefficients were used to check the published spectra. Reported absorption spectra were also compared to measured spectra on the

samples tested for optical cooling as discussed in the next section. For anisotropic materials, polarized emission data were averaged to compute λ_F and the pump and laser polarizations were selected to optimize the figures-of-merit. For a few materials, no reports of the manifold energy levels were found in the literature. In these cases, the room temperature partition functions were approximated as unity. Numerical studies on the well-known materials revealed that this approximation only weakly impacts the results of the calculations.

Note the wide range of values for the figures-of-merit that these materials exhibit. This is because RB lasers are very sensitive to the shape as well as the magnitude of the red wing spectral data. Broad spectral bands and high cross sections are very favorable. Based on this spectral analysis, we predict that Yb^{3+} doped $\text{KY}(\text{WO}_4)_2$ and $\text{KGd}(\text{WO}_4)_2$ will exhibit superior laser performance in RB laser systems. They exhibit figures-of-merit nearly an order of magnitude higher than any other material considered. These predictions are based on the assumption that the materials can exhibit near unity quantum efficiency in practice. The validity of this assumption is tested in the next section.

Anti-Stokes Optical Cooling Experiments

In order to determine actual quantum efficiencies, a photothermal deflection spectrometer was constructed using a tunable titanium-sapphire laser as the pump source and a helium-neon laser as the probe. The cw pump source was chopped at a slow rate and focused into a sample material. The helium-neon probe beam counter-propagates through the sample and is slightly deflected by the thermal transient. Deflections are measured several meters away on a large-area dual-cathode silicon diode. With minimum vibrations and air turbulence, angular deflections as small as $0.01 \mu\text{rad}$ could be resolved. A small diameter probe beam ($50 \mu\text{m}$) ensures that the photothermal deflection is not sensitive to radiation trapping inside bulk samples. Tuning of the pump source allows for direct determination of the heat generated by the pump absorption. As the pump beam is tuned to longer wavelengths the amplitude of the deflection decreases. Optical cooling is indicated by when the transient deflection decreases to zero and then changes sign. Used in this way, the photothermal deflection technique can detect small deviations from ideal radiative decay.

Photothermal deflection experiments were conducted on high quality samples of lightly ytterbium doped $\text{Y}_3\text{Al}_5\text{O}_{12}$ (YAG), LiYF_4 (YLF), $\text{KGd}(\text{WO}_4)_2$ (KGW), and ZBLANP glass. Chopping of the pump beam for 50 milliseconds produced a transient deflection of the HeNe probe. The peaks of the transient deflection signals were recorded while the pump was tuned over a range of 940 to 1030 nm. Incident pump power was recorded since it also varied during the tuning. Absorbed power density was computed from the incident power and measured absorption spectra. Optical cooling was observed for long wavelength pumping of the samples of KGW and ZBLANP, while only heating was observed for the YAG and YLF samples. Weak green fluorescence at 530 to 560 nm was visible in all samples, indicating some level of residual impurities, possibly erbium.

When the measured photothermal deflection signals are normalized by the absorbed pump power, they yield a number proportional to the internal heat generation rate of the material. Plotting this normalized signal in Fig. 1, the spectral dependence of the internal heat generation is revealed. Mungan and Gosnell have shown that this type of data can be analyzed using a simple rate equation model [6]. This model includes steady state excitation and spontaneous emission of the $\text{Yb}^{3+} \text{}^2\text{F}_{5/2}$ level. To account for possible heating due to nonradiative decay routes, they included a background nonsaturable pump absorption coefficient, α_b , and a direct linear quenching power per ion, κ . According to the model, the spectral dependence of the rate of laser-induced heating, $\dot{\rho}$, is given by

$$\frac{\dot{\rho}}{I_p} = \left(1 - \frac{\lambda_p}{\lambda_F} + \frac{\kappa\tau\lambda_p}{hc} \right) \alpha(\lambda_p) + \alpha_b, \quad (13)$$

where I_p is the unsaturated pump intensity and $\alpha(\lambda_p)$ is the Yb^{3+} absorption coefficient. Let λ_0 represent the wavelength of the photothermal deflection crossover from heating to cooling. The degree of nonradiative decay in a particular sample can then be quantified by the fractional shift in the actual deflection crossover from that of an ideal radiator, λ_F ;

$$\frac{\lambda_0 - \lambda_F}{\lambda_F} = \frac{\alpha_b}{\alpha(\lambda_0)} + \frac{\kappa\tau\lambda_0}{hc}. \quad (14)$$

In words, the fractional shift in the crossover wavelength is simply equal to the sum of the ratio of the background to the ytterbium absorption plus the fraction of excited ytterbium ions that decay via quenching.

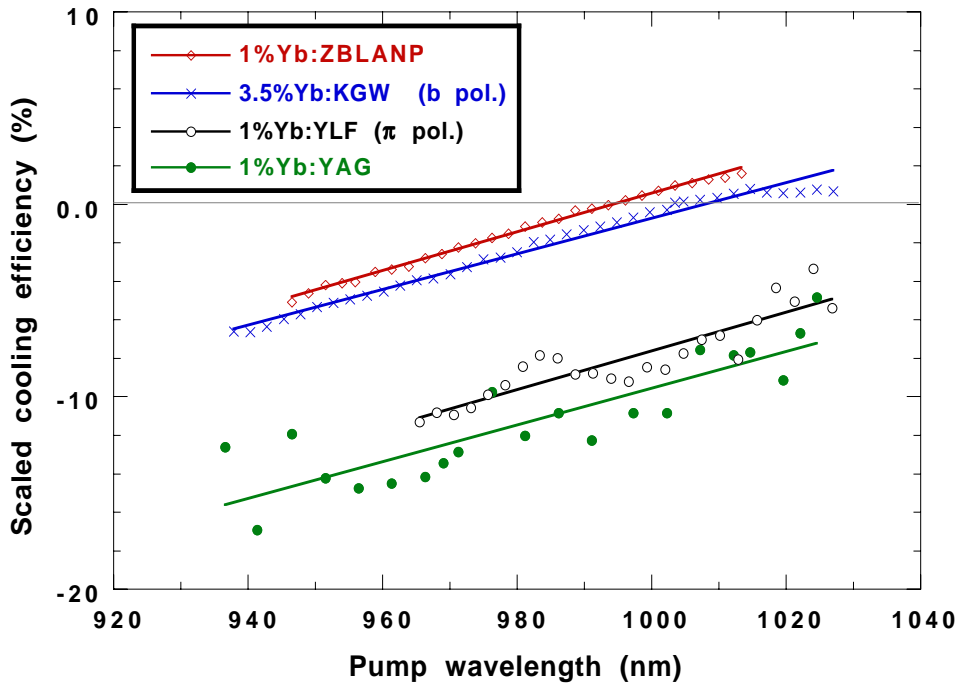


Figure 1. Normalized deflection signal as a function of pump wavelength. Negative signals indicate heating, while positive signals indicate cooling. The pump polarization is indicated in parentheses for the anisotropic samples.

Figure 1 illustrates the usefulness of this technique for evaluating material quality. The samples of ZBLANP and KGW exhibit 0.0% and 1.6% degrees of nonradiative decay, respectively. The value for KGW is uncertain to within 0.5% because of potential inaccuracies in the spectral data of this relatively new biaxial material. Fluorescence and absorption spectra of the other materials are better known and therefore estimates of the actual mean fluorescence wavelength, λ_F , are more reliable. Extrapolating the deflection crossovers for the YLF and YAG samples in Fig. 1 yield estimates of 8.0% and 9.2% degrees

of nonradiative decay, respectively. These are significant heat generation rates, even for conventional Yb³⁺ laser systems. Clearly, further work on material refinement will be required to identify this loss mechanism and improve these laser materials.

Summary

Optimal performance criteria are derived for steady state radiation balanced lasers. A spectral analysis of selected ytterbium doped materials reveals KY(WO₄)₂ and KGd(WO₄)₂ to be the most promising. These crystals have figures-of-merit an order of magnitude higher than those of Yb:YAG, the most widely used 1.03 μm laser material. Optical pumping experiments confirm the potential of these tungstate materials. Anti-Stokes cooling is reported at room temperature in 3.5% Yb doped KGd(WO₄)₂ crystals. Initial as-obtained samples of this material exhibited a 98.4% radiative quantum efficiency. This is the first report of optical cooling in a crystal and the first step towards the demonstration of a new class of very high power solid-state lasers.

Acknowledgment

This work was supported by the Office of Naval Research. We also thank T.R. Gosnell for valuable discussions and for the loan of the ZBLANP sample used in this study.

References

1. P. Pringsheim: *Z. Phys.* **57**, 739 (1929).
2. N. Djeu and W. T. Whitney: *Phys. Rev. Lett.* **46**, 236 (1981).
3. Christoph Zander and Karl Heinz Drexhage: in *Advances in Photochemistry*, vol. 20, edited by D. C. Neckers, D. H. Volman, and G. von Büнау (Wiley, New York 1995).
4. J. L. Clark and G. Rumbles: *Phys. Rev. Lett.* **76**, 2037 (1996).
5. Richard I. Epstein, Melvin I. Buchwald, Bradley C. Edwards, Timothy R. Gosnell, and Carl E. Mungan: *Nature (London)* **377**, 500 (1995).
6. Carl E. Mungan and Timothy R. Gosnell: *Adv. At. Mol. Opt. Phys.* **40**, 161 (1999).
7. Steven R. Bowman: *IEEE J. Quantum Electron.* **35**, 115 (1999).
8. N. V. Kuleshov, A. A. Lagatsky, V. G. Shcherbitsky, V. P. Mikhailov, E. Heumann, T. Jensen, A. Dening, and G. Huber: *Appl. Phys. B* **64**, 409 (1997).
9. N. V. Kuleshov, A. A. Lagatsky, A. V. Podlipensky, V. P. Mikhailov, and G. Huber: *Opt. Lett.* **22**, 1317 (1997).
10. Material data sheets on Yb:KY(WO₄)₂ and Yb:KGd(WO₄)₂ from Thor Labs Inc.
11. D. S. Sumida, T. Y. Fan, and R. Hutcheson: *OSA Proceedings on Advanced Solid-State Lasers Vol. 24*, Bruce H. T. Chai and Stephen A. Payne, eds. (Optical Society of America, Washington, D.C., 1995).
12. Laura D. DeLoach, Stephen A. Payne, Wayne L. Kway, John B. Tassano, Sham N. Dixit, and William F. Krupke: *J. Lumin.* **62**, 85 (1994).
13. Stephen A. Payne, Laura D. DeLoach, Larry K. Smith, William F. Krupke, Bruce H.T. Chai, and George Loutts: *OSA Proceedings on Advanced Solid-State Lasers Vol. 20*, T. Y. Fan and Bruce H. T. Chai, eds. (Optical Society of America, Washington, D.C., 1994).
14. Stephen A. Payne, Larry K. Smith, Laura D. DeLoach, Wayne L. Kway, John B. Tassano, and William F. Krupke: *IEEE J. Quantum Electron.* **30**, 170 (1994).

15. Hans W. Bruesselbach, David S. Sumida, Robin A. Reeder, and Robert W. Byren: *IEEE J. Selected Topics Quantum Electron.* **3**, 105 (1997).
16. Kathleen I. Schaffers, Laura D. DeLoach, and Stephen A. Payne: *IEEE J. Quantum Electron.* **32**, 741 (1996).
17. Laura D. DeLoach, Stephen A. Payne, L. L. Chase, Larry K. Smith, Wayne L. Kway, and William F. Krupke: *IEEE J. Quantum Electron.* **29**, 1179 (1993).
18. Pu Wang, Judith M. Dawes, Peter Dekker, David S. Knowles, James A. Piper, and Baosheng Lu: *J. Opt. Soc. Am. B.* **16**, 63 (1999).
19. L. Fornasiero, E. Mix, V. Peters, K. Petermann, and G. Huber: *Cryst. Res. Technol.* **34**, 255 (1999).
20. B. Simondi-Teisseire, B. Viana, D. Vivien, and A. M. Lejus: *Phys. Stat. Sol. (a)* **155**, 249 (1996).
21. F. Mougel, K. Dardenne, G. Aka, A. Kahn-Harari, and D. Vivien: *J. Opt. Soc. Am. B.* **16**, 164 (1999).
22. D. A. Hammons, L. Shah, J. Eichenholz, Q. Ye, M. Richardson, B. H. T. Chai, A. Chin, and J. Cary: *OSA Proceedings on Advanced Solid-State Lasers, Vol. 26*, Martin M. Fejer, Hagop Injeyan and Ursula Keller, eds. (Optical Society of America, Washington, D.C.,